PORT SAID ENGINEERING RESEARCH JOURNAL
Faculty of Engineering - Port Said University
Volume 27 No. 3 pp: 70-88

Removal of Cationic Dyes from Water by Using Nano Adsorbents Sulfonated Carboxy Methyl Cellulose: (Characterization, Isotherm, Kinetics and Thermodynamics)

R.E. Khalifa[1], Moustapha Salem Mansour[2], Ebrahim Esmail Ebrahima[3], Ibrahim Ashour[4], Mohamed S. Elgeundi[5], Hadier R. Ashour[6,]*

[1] *polymer Materials Research Department, Advanced Technologies Institute, City of scientific Research and Technological Applications, New Borg El-Arab City, email: randaghonim@gmail,com*

[2] *Chemical Engineering Department, Faulty of Engineering, Alexandria, Egypt, email: mansourms@alexu.edu.eg*

[3] *Chemical Engineering Department, Faulty of Engineering, Minia, Egypt, email: prof.ebrahiem@mu.edu.eg*

[4] *Chemical Engineering Department, Faulty of Engineering, Minia, Egypt, email: Ibrahim.ashour@mu.edu.eg*

[5] *Chemical Engineering Department, Faulty of Engineering, Minia, Egypt, email: elgandy1949@yahoo.com*

[6] *Alexandria Higher Institute of Engineering and Technology, Basic Science Department, Alexandria*

**Corresponding author, hadier.ragab@aiet.edu.eg,DOI: 10.21608/PSERJ.2023.195709.1223*

Received 27-2-2023
Revised 20-5-2023
Accepted 15-6-2023

ABSTRACT

In the following study, preparation of nano adsorbent from carboxymethyl cellulose (CMC) was carried out by introducing sulfonate group on CMC to prepare sulfonated carboxy methyl cellulose (SCMC). The polymer was used for adsorptive cationic dye removal models: crystal violet (CV) and methylene blue (MB). The produced nanostructure and morphology of the SCMC were investigated by Transmission Electron Microscopic (TEM), Zeta potential, Fourier transform infrared (FT-IR) spectroscopic analyses, and scanning electron microscopy (SEM). The spectrophotometric study of the adsorption properties of SCMC for removal of both cationic dyes was conducted as a function of contact time, solution pH, initial dye concentration, temperature, and adsorbent dosage. The maximum adsorption capacities of the SCMC nanoparticle-based adsorbent for both MB and CV were described by the data on the equilibrium adsorption of both cationic dyes, which fitted well with the Langmuir model (R^2 = 0.998 for MB dye) but for CV the equilibrium data fitted well with Elovich model (R^2 =(0.9961). The kinetics of adsorption followed the pseudo-first-order model. The adsorption process is endothermic, and spontaneous; according to thermodynamic studies conducted at temperatures ranging from 298 to 313 K. When the parameters are tuned, the adsorbent can remove both dyes quickly and with a high level of efficiency.

Keywords: Adsorption, Methylene Blue, Crystal Violet, Nano Adsorbent, Isotherms, Kinetics.

1. INTRODUCTION

Water contamination has become a huge problem for humans and the environment as a result of technological progress. As a result of increased industrialization, harmful organic pollutants that haven't been handled have been released directly to water, affecting the water's quality and aquatic life[1] Metals, phosphate, pathogens, organic matter, hydrocarbons, and dyes are the principal contaminants in wastewaters.[2] Dyeing wastewater is characterized by a high volume, complex components,

and high toxicity, so its treatment has garnered the interest of different researchers. [3]

Multiple industries, including paper, textiles, plastic, ink, paint, ink [4], rubber, leather, food, and cosmetics[2] a variety of organic dyes are utilised, with approximately 15% being lost during synthesis and processing with wa stewater.[4] Including synthetic colors, industrial waste effluent has many hazardous compounds that harm human health and the environment. [5] Methylene blue (MB) (C16H18ClN3S) is the most widely used dye for colouring cotton, silk, and wood. It can cause nausea, profuse, vomiting, red blood cell destruction, and methemoglobinemia.[6] Also, crystal violet (CV) (C25N3H30Cl) is a much more lethal form of triphenylmethane dye. The complex aromatic structures and physicochemical features of CV dye give it excellent thermal, chemical, and light stability.[6] Crystal violet is an industrial dye used as a biological stain and, in the production of dyes, belongs to the triphenylmethane family of dyes. Most members of this huge family are known to be carcinogenic and mutagenic, despite their widespread use in industrial applications. It is believed that the presence of CV in the water system represents a danger to human health.[5]

A number of effective wastewater treatment methods for removing such contaminants were investigated. Chemical oxidation, electrochemical treatment, reverse osmosis, ozonation, nanofiltration, advanced oxidation processes,[6] aerobic processes, coagulation, anaerobic processes, flocculation[7], biological techniques, membrane filtration, and adsorption [4]. Among these, the adsorption method one of the most often utilised methods in dye-related sector such as coating, wool, paint, and textiles, with the primary purpose of removing dye residue from effluent.[7] The advantages of the adsorption method are low cost, easy operation, high safety, and high pollutant removal efficiency. The effectiveness of adsorption removal depends on the functional group properties of the adsorbate molecules (molecular size, functional groups). Structure and morphology of the adsorbent's surface (specific surface area, surface charge, and functional group).[8] Adsorption technology, including porous solids with a large surface area, is used to remove contaminants from liquid or gas effluents.[9] Nanomaterials with dimensions between one and one hundred nanometers have a number of benefits, including an increase in surface bulk volume ratio and surface area. This results in the effective cleansing of waste water. [10]

Clay, activated carbon, and mesoporous materials are among the several adsorbents exploited in the purificatio n of coloured waters that are described in the scientific lit erature, [11] bentonite, activated alumina, charcoal, and zeolites. They also have problems like a short useful life, a high consumption rate, and a hard time regeneration. So, it is important to make new adsorbents that are very useful. Cellulose is a naturally occurring polymer that can be found in wood, cotton, cotton linters, wheat, straw, reads.[12] The annual production of cellulose is anticipated to exceed 7,510 metric tons. The hydroxyl groups on the cellulose molecule give locations for chemical alteration to improve the electrochemical interaction of cellulose with other molecules, hence enhancing adsorption capacity.[13] Carboxymethyl cellulose (CMC) is a main cellulose byproduct that is tasteless, odorless, soluble in water, and non-toxic.[14] NaCMC is a polysaccharide composed of water-soluble cellulose derivative containing carboxymethyl groups bonded to hydroxyl groups of glucopyranose monomers. Due to their superior protective capabilities and eco-friendliness, cellulose and its derivatives have been utilized in several domains, such as corrosion inhibitors and multidrug-resistant illnesses, in recent years.[15] The addition of various functional groups can increase the adsorption capacity of polymeric nanoparticles by facilitating contact between the nanoparticles and different locations on contaminating molecules (such as dyes).[16]

The purpose of this effort is to investigate the impact of modified CMC (sulfonate carboxy methyl cellulose) as nano adsorbent on the removal of both cationic dyes (MB& CV) from water. The adsorption-influencing parameters, including adsorbent dosage, initial dye concentration, temperature, pH, and contact time, were optimized for maximal dye removal from the aqueous solution. The modified CMC was characterized using transmission electron microscopy (TEM), zeta potential, Fourier transform infrared (FT-IR) spectroscopy, and scanning electron microscopy (SEM).

2. MATERIALS AND METHODS

2.1 Materials

Sodium Carboxy Methyl Cellulose (NaCMC) low viscosity (ADWIC, pure lab. Chemicals), Sodium sulfite, Ethanol (made in Germany), Epichlorohydrin (ECH) C3H5CLO (LOBA Chemie). The most common contaminants are the cationic dyes Methylene blue (MB) and Crystal violet (CV). Table 1 lists the molecular and chemical formulas as well as further details on both colors. [17] Hydrochloric acid (HCl) Sodium hydroxide (NaOH) and were employed to regulate the pH during batch tests designed to determine the effect of processing factors.

Table 1. C.F, M.F, and M.P for both dyes (MB) and (CV).

Properties of both dyes	Crystal Violet (CV)	Methylene Blue (MB)
C.F	$C_{25}H_{30}ClPN_3$	$C_{16}H_{11}ClPN_3S$
M.F	408 g/mol	319.85 g/mol
M.P	205^0C	100-110^0C

2.2 Preparation of Sulfonate Carboxy Methyl Cellulose (SCMC)

Prepare a mixture by preparing a solution of 2% CMC low viscosity (dissolve 2 g CMC in 80 ml H2O) to 0.5 ml epichlorohydrin (ECH) and stirring them for 2 hours at room temperature. Then add 0.4 ml ECH and a solution of sodium sulfite (dissolve 3 g in 20 ml H2O). After that, the mixture refluxed on a water bath at 550 for 2 hours and cooled. The product was precipitated in ethanol, filtered, and then dried at 500 C over night. Finally, the final product was converted into nanoparticles using a ball mill.

2.3 Characterization Studies

Using Fourier Transform Infrared Spectroscopy, the chemical structure of the produced adsorbent was analyzed (FTIR, BRUKER, TENSOR 37 spectrometer). Using scanning electron microscopy (SEM), the physical characteristics of SCMC adsorbent surfaces were investigated (JEOL JSM-6010LV). Changes in the surface morphology of the produced adsorbent were analyzed using Transmission Electron Microscopy (TEM) (JEOL JTM-1400), Japan, and the zeta potential was determined using Transmission Electron Microscopy (TEM) (MALVERN, ZETASIZER, Nano-ZS).

3. RESULTS AND DISCUSSION

3.1 Fourier Transform Infrared (FT-IR)

Fourier transform infrared (FTIR) spectroscopy was utilized to determine the surface functional groups of modified cellulose sulfonate carboxy methyl cellulose (SCMC). As shown in Fig. 1.a, the peak at 3432 cm-1 in the FTIR spectrum of CMC is owing to the stretching vibration of the (OH) groups of

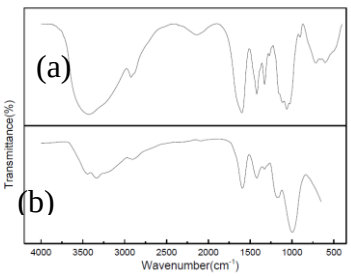

Figure 1: FTIR (a) CMC and (b) SCMC

cellulose. [18] Additional peaks at (2923 cm-1 and 1422 cm-1 and 1599 cm-1) correspond to (C-H), (COO), and (C=C) bonds, respectively.[19] By addition of sulfate group a new sharp peak appear at (900-1100 cm-1) was due to -SO4 group[20] and decrease in the other peaks at 3340,2923,893 cm-1 for -OH,C-H and C=O group, respectively. And decrease in vibration motion at peak 1186-1588 cm-1for C=C bond. According to FTIR analysis the shift in OH, C=O may be due substitution of some of the hydroxyl groups with other functional groups, such as sulfonate and some of the original carbonyl groups in the cellulose structure have been modified or removed[6]. Overall, the decrease in these peaks suggests that significant modifications have been made to the cellulose structure in the SCMC sample.

3.2 Scanning Electron Microscopy Analysis (SEM)

The morphology of the produced adsorbents and the nature of the utilized polymers can greatly impact the adsorption capabilities of SCMC (Sodium carboxymethyl cellulose) nanoparticles. Sulfonate groups are hydrophilic and can form strong hydrogen bonds with water molecules, which can increase the solubility and dispersibility of the NaCMC particles in water. This can lead to a more uniform distribution of the particles in the aqueous solution. As demonstrated in Figure 2 (a), the morphological structure of the produced adsorbents and the natively utilized polymers was studied using SEM. The surface of native CMC was characterized by an irregular granular surface.[10] In Fig.2 (b) it is noticeable that the surface of MMT is compact and flat, exhibiting crystal characteristics.

Nanoparticles of SCMC have numerous pores and a large surface area, and there is a strong chance that dyes will be absorbed into these pores.[21] The morphology of the adsorbents plays a significant role in determining the surface area and pore size distribution of the adsorbent. A larger surface area and a narrow pore size distribution can enhance the adsorption capacity of the adsorbent, as it provides more surface area for the adsorption of the target molecule and a more uniform pore size distribution, allowing for more efficient access to the active sites on the surface of the adsorbent.[22] The well-dispersed pattern of sulfonate groups in NaCMC molecules can also be an indication of the average particle size. In general, smaller particles tend to be more uniformly dispersed in solution compared to larger particles. [23]

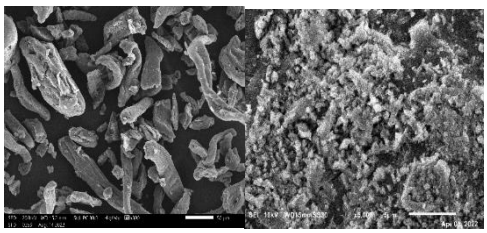

Figure 2: SEM analysis (a)CMC and (b)SCMC.

3.3 Transmission Electron Microscopy (TEM) Analysis

Fig. 3 shows the TEM microphotograph of the SCMC nanoparticles. Almost all the sulphonate groups are well dispersed in the NaCMC molecules,[21] the

TEM results also suggest that the average particle size was between (1.63 and 10.46 nm). Due to SCMC's aggregation behavior, rough surface layer interfaces can be significantly improved.More SCMC increases su rface irregularity and nano-size uniformity.[24]

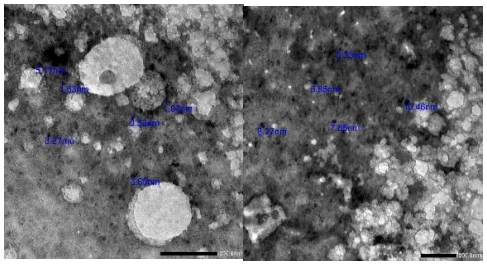

Figure 3: TEM analysis for SCMC.

3.4 Surface Characterization of SCMC

At pH 7, the zeta potential of the investigated SCMC was measured and found to be -44.6 mV. When the total charge on as adsorbent's surface is zero and the zeta potential is also zero, the surface is said to be neutral. pH is measured in terms of the point of zero charge (pHPZC)**.**[25]

3.5 Reusability Test

Adsorption-desorption cycles were used to investigate the reusability of the prepared SCMC for MB and CV adsorption.

After the adsorption process was complete, the adsor bed dye was isolated from the batch adsorption runs and immersed in a desorption agent solution (50 mL) contain ing 1 M HCl. [10]

3.6 Studies on Point of Zero Charge (pHzpc)

pHzpc was studied adjusting 0.01 M NaCl's pH to 2–12 using NaOH or HCl. Then, 0.05 g of adsorbent was added to 10 mL of 0.01 M of NaCl in conical flasks. pH was measured after 24 hours in the flasks. (pHfinal-pHinitial) vs. pH initial graphs were then drawn. [26]

3.7 Effect of Initial Dye Concentration and Contact Time

The influence of contact time on the elimination of cationic dyes is seen in Fig. 4 when the studies are conducted using solution with concentration of 30 mg/L with 0.05 g of nanoparticles of SCMC adsorbent at 298 K and pH 7. The favorable interaction between the anionic sulfonate group and the cationic methylene blue dye results in higher dye removal capability at the first stage. As the adsorption process progresses, dye molecules partially or completely cover the adsorbent's surface, resulting in decreased absorption. [27]

Fig. 5 illustrates the effects of starting solution concentration on MB and CV elimination and dye absorption (qt) at 298 K for concentrations from 10 to 100 mg. L-1, 0.05 g SCMC nanoparticles as adsorbent, and pH 7. The results reveal that CV and MB dye removal from water decreases with increasing of solution dye concentration.[17] MB was eliminated from (91.41 to 49.9) and CV from (98.1 to 47.7). Nano adsorbents may have huge active sites that can bind dyes at low concentrations but become saturated at high doses.[19]

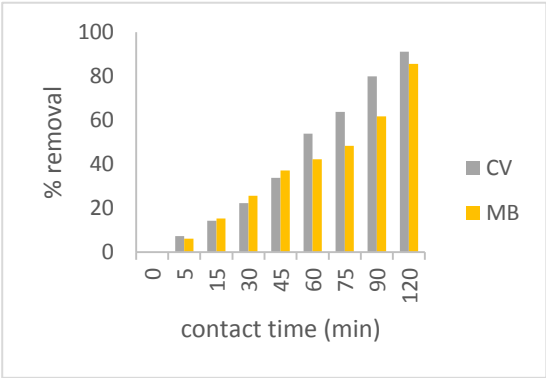

Figure 4: Effect of contact time on MB and CV removal (initial concentration 30 ppm, temperature 25^0 C, pH=7, adsorbent dose=0.05g).

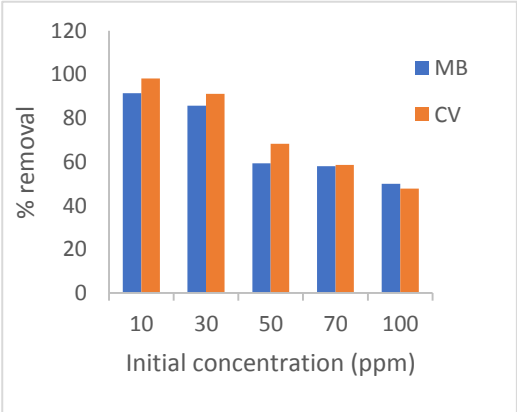

Figure 5: Effect of initial concentration on MB and CV removal (temperature 25^0 C, pH=7, adsorbent dose=0.05g).

3.8 Effect of Adsorbent Dose

Due to an increase in adsorption site and surface area, the proportion of dye that is removed rises as adsorbent dosage increases. Adsorption behavior is determined by the amount of sorbent used. In order to achieve this result, we used SCMC nanoadsorbent in different doses, dyes at 30 ppm, pH 7, and 120 min of contact duration.[28] As shown in Fig.6 For MB, this increased

from 85.6 to 93.6, while for CV, it went from 91.1 to 98.59. However, at large adsorbent dosages, the removal percentage rose slowly, demonstrating that dye adsorption equilibrium had already been achieved.

Initially, increasing the adsorbent dosage increased the removal of both cationic dyes.[29]. At first, the nanoadsorbent's surface has a lot of active sites that help dyes penetrate it, but as the amount of adsorbent rises, more particles become agglomerated on the MB and CV surfaces, which slows down the adsorption process somewhat.[19]

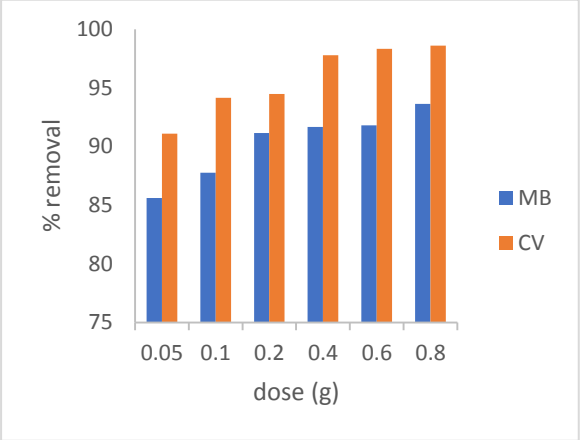

Figure 6: Effect of SCMC dosage on MB and CV removal (initial concentration 30 ppm, temperature 25^0 C, pH=7).

3.9 Effect of Temperature

One of the most critical elements impacting adsorptio n behaviour is temperature. The effect of process temperature on the proportion of elimination cationic dyes by using nanoparticles of SCMC was investigated at (298, 303, and 318 K), an initial concentration of MB and CV of 30 ppm, an amount of nano SCMC of 0.05 g, and a solution pH of 7. Figure 7 shows that the amount of adsorbed CV and MB increased when the temperature was elevated. This might be because when the temperature rises, there is a greater diffusion of dye molecules and a large number of active sites grow on the surface of nano SCMC. However, beyond a certain temperature, the saturation of the adsorbent surface with both dye molecules (MB and CV) may lead to a minor rise in the percentage of dye removal.[10]

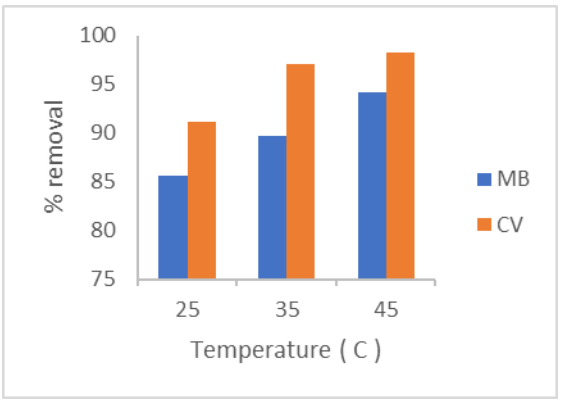

Figure 7: Effect of different temperature on MB and CV removal (initial concentration 30 ppm, adsorbent dose 0.05 g, pH=7).

3.10 Effect of pH

One of the most important things to look at is the pH of the solution. that determines the overall adsorption rate. Using 0.05 g of adsorbent, an initial concentration of 30 ppm, and a temperature of 298 K, the effect of solution pH on the elimination of MB and CV dyes from an aqueous solution was investigated by varying the range from 3 to 11. As shown in Figure 8 The end point of the pH is where the curves meet the hor izontal line. This point has a value of 7. If pH is below pH zpc, the surface charge of the adsorbent goes up (positive), and if pH is above pH zpc , the surface charge goes down (negative). [26] As seen in Figure 9, the clearance of MB&CV first increases as pH increases but decreases as pH increases further.[30] In the presence of an acidic solution, the collision between positive ions and cationic dyes reduces the adsorption between the

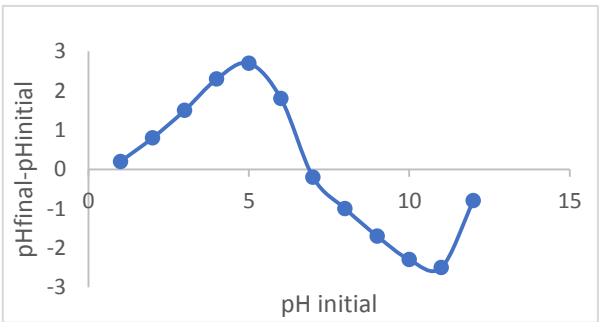

Figure 8: pHpzc of SCMC

cationic dye and the nanoparticle adsorbent due to the high concentrations of H+ ions.[17] At high pH, the concentration of (OH-) ions in a solution increases. In this instance, the cationic dyes react with the (OH-) ions in the solution to form complexes rather than adsorbing on the nanoparticle PCMC surface, hence decreasing the adsorption rate.[31]

4. EQUILIBRIUM ISOTHERMS

100 mL of DW (H_2O) were used to dissolve 0.1 g of each dye. a stock solution of 1000 ppm (mg/L) of CV and MB was created, and the desired concentration was obtained by dilution.[6]

The kinetics of adsorption, thermodynamics, and isot herms were studied. The initial and final concentration of solution containing dye (MB and CV) were measured before and after adsorptions. The capacities of adsorption at time t and adsorption rates for dyes estimated by the following Equations(1 and 2):[6]

UV–Visible spectroscopy was used to calculate the final dye concentrations (absorbance).[11]
Adsorption performance was determined by (qt) using the following equations:

$$q_t = \frac{(C_0 - C_t) * V}{m} \quad (1)$$

$$q_e = \frac{(C_0 - C_e) * V}{m} \quad (2)$$

Where qt is the amount of cationic dye adsorbed (g) of adsorbent at time (t) (mg.g-1) and qe is the equilibrium adsorption capacity (mg.g-1) and C0, Ct, and Ce are dye concentration at time zero, and time (t) (mg.l-1), and equilibrium dye concentration (mg.l-1), with (V) being the volume of solution (mL) and (m) being the mass of nano adsorbent (g).[11]
The %removal of dye was calculated by equation (3).[6]

$$\%removal\ of\ dye = [\frac{(C_0 - C_t)}{C_0}] * 100 \quad (3)$$

4.1 Adsorption Isotherms

The adsorption isotherms of crystal violet and methylene blue by nano-Sulfonate carboxymethyl cellulose were investigated by five mathematical models: Langmuir's isotherm, [25] Freundlich's isotherm, [11] Temkin model, D-R model, and Elovich model, which were used to determine R^2 (correlation coefficient).

4.1.1 Langmuir Isotherm

The Langmuir theory is based on the ideas that the surface is uniform, that the adsorbed molecules don't interact with each other, and that the surface has many places where molecules can stick to it. The linear form of Langmuir is shown in the following equations.[32]

$$q_e = \frac{q_m K_L C_e}{1 + K_L C_e} \quad (4)$$

$$\frac{1}{q_e} = \frac{1}{K_L q_m C_e} + \frac{1}{q_m} \quad (5)$$

And $R_L = \frac{1}{1 + K_L C_0}$ (6)

where K_L represents the Langmuir constant in $L.mg^{-1}$, q_e represents the equilibrium adsorption capacity in $mg.g^{-1}$, q_m represents the maximum adsorption capacity in $mg.g^{-1}$, C_e represents the equilibrium concentration of solution in $mg.L^{-1}$, and R_L represents the separation factor computed from equation (6).

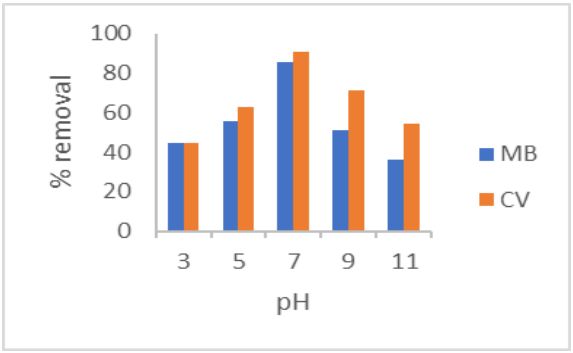

Figure 9: Effect of pH on MB and CV removal (initial concentration 30 ppm, adsorbent dose 0.05 g, temperature 25^0 C).

R_L show whether or not the process of adsorption is a go od one. If R_L = 1, the process is linear. If R_L 1 is present, the process is favorable. If R_L>1, the process is not favorable. If R_L=0, the process is reversible.[20] By plotting (1/qe) against (1/Ce), as shown in Figs. 10(a) and 11(a) for MB and CV, respectively, we can obtain a straight line relation with a slope of ($1/K_L qm$) and intercept of (1/qm), and we can obtain an R2 value correlation coefficient of R^2 = 0.998 and 0.9332 for methylene blue and crystal violet, respectively. The data for both dyes were listed in Table (2). Also can determined the value of q_{max} value is ($45.24887 mg \cdot g^{-1}$, 43.10345 mg.g-1) and the value of K_L which equal (0.272503 L.mg-1 , 0.470588 L.mg-1). The values of RL for all concentrations (10–100 mg/l) of MB between (0.259150421 and 0.037345039 $mg.l^{-1}$) and R_L values of CV at different concentrations between (0.168440191 and 0.020326524 $mg.l^{-1}$) consider the fact that adsorption is more favourable and conclude that a monolayer is forming during theadsorption of MB and CV onto the surface of SCMC.

4.1.2 Freundlich Isotherm

Based on the Freundlich isotherm, adsorption happened on a surface that has different types of molecules on it.

his is true for both monolayer (chemisorption) and m ultilayer (physisorption) adsorption.[33].The nonlinear and linear equation as follow

$$q_e = K_f C_e^{\ 1/n} \quad (7)$$

$$log(q_e) = log K_F + \frac{1}{n} log(C_e) \quad (8)$$

Where q_e is the adsorption capacity at equilibrium, mg/g; K_F is the Freundlich constant; C_e is the equilibrium concentration, mg/L; n is the intensity of adsorption. As shown in Fig.10 (b), 11(b) by graphing log qe vs log Ce

the slope and intercept can calculated. K_F quantifies the amount of dye adsorbed onto an adsorbent and indicates the bonding energy and/or distribution coefficient.1/n represents adsorption intensity, with values ranging from 0 to 1.

When the value of 1/n equals 1, the adsorption is linear; when it is less than 1, the adsorption is chemically driven; and when it is greater than 1, the adsorption is physical.[33]The values of 1/n (0.31 and 0.245) for MB, CV give an indication of how well adsorption will work and high tendency of MB and CV for the adsorption onto SCMC. Each parameter is detailed in Table (2).

4.1.3 Temkin Isotherm

The Temkin isotherm is based on the assumption that the free energy of sorption is proportional to the surface covering. Over the surface of SCMC applied at room temperature, the linear form is stated as shown in Equation (9)[32]

$$q_e = BlnA_T + BlnC_e \quad (9)$$

Where

$$B = {}^{RT}/_{b} \quad (10)$$

In this model B is the heat of adsorption (J mol-1); AT (L/g) is the equilibrium binding energy for Temkin model. By plotting qe against (ln Ce) as shown in Fig.10 (c), 11 (c) to obtain the slope (B) and intercept (BlnAT).

R is the gas constant (8.314 J/mol K), and T is the temperature. If constant B is positive (J/mol), it means that MB and CV are going through a process that uses up heat..[32] The value of the correlation coefficient R^2 (0.907 and 0.947) for MB and CV respectively.

4.1.4 Dubinin-Radushkevich Isotherm (DKR)

The Dubinin-Kaganer-Radushkevich(DKR) model has been utilized to assess the adsorbent's porosity characteristics and the adsorption process' energy.
The DKR equation takes the following form: [34]

$$ln\, q_e = ln\, q_D - 2B_D RT\, ln(1 + {}^{1}/_{C_e}) \quad (11)$$

And

$$E_{D-R} = \sqrt{{}^{1}/_{2\,B_D}} \quad (12)$$

Where R, is the gas constant (0.08314 KJ/mol·K); T absolute temperature (K) ; q_D and B_D are the constants of Dubinin-Radushkevich model obtained from slope and intercepet of plotting (lnq_e) against (ln (1+1/C_e))as shown in Fig.10 (d) ,11 (d).In Table (2), The value of E_{D-R} shows if the process of adsorption is physical or chemical.The fact that the E_D values were equal (0.280872 and 0.208741 kJ/mol for both colours) suggested that the adsorption process was chemical adsorption of dye molecules.[35]

4.1.5 Elovich Isotherm

The equation of the Elovich model defines the adsorption process as follows:

$$ln\frac{q_e}{C_e} = ln(K_E\, q_m) - \frac{1}{q_m} q_e \quad (13)$$

The slopes and intercepts of the linear plot between ln (qe/ce) vs qe, where K_E is the equilibrium constant (L mg^{-1}) and q_m is the Elovich maximum adsorption capacity (mg/g), can be used to determine the value of this term, as shown in Fig.10 (e), 11 (e) yield a linear correlation coefficient (0.9383 and 7.788162) for MB and CV. Table (2) summarise the estimated parameters from isotherm models.

The regression coefficient (R^2) for the Langmuir isotherm is near unity for MB adsorption on the surface of SCMC as a nanoadsorbent (0.998). Dissimilar adsorption models have lower correlation coefficient that pertinent models, with Langmuir (0.998) coming first, followed by Freundlich (0.9681), Elovich (0.9383), Temkin (0.907), D-R (0.8978). And the Elovich isotherm model fits the best for CV adsorption on SCMC. The R^2 values for Elovich (0.9961), Freundlich (0.9896), Temkin (0.9472), Langmuir (0.9332), and D-R are as follow: (0.7751).

4. ADSORPTION KINETICS

Using pseudo-first-order, pseudo-second- order, and Elovich models, we examined the adsorption kinetics of cationic dyes (MB and CV) on the surface of nano particles of SCMC.[25] The experimental results for both dyes were analyzed at varying starting concentrations and temperatures. Following is the linear form for pseudo-first order:[36]

$$log(q_e - q_t) = log\, q_e - \frac{K_1}{2.303} t \quad (14)$$

where qe and qt represent the amount of dye adsorbed (mg/g) at equilibrium time t and time t, respectively (min). K_1 was calculated from the slope of the log (qe-qt) versus t[36] plots in Figs. 12; 15, 18; and 21, and the kinetic parameters were listed in Table 3.

The following equation represents the pseudo-second-order model's linear form:

$$\frac{t}{q_t} = \frac{1}{K_2 q_e{}^2} + \frac{t}{q_e} \quad (15)$$

Where K_2 is the adsorption equilibrium constant determined by the intercept of the linear relationship between t/qt and t, as shown in figs. 12, 15, 18, and 21, and qe, which is determined by the slope. The table displayed the kinetic parameters (4).

The linear form of Elovich model as follow:

$$q_t = (\frac{1}{\beta})\, ln(\alpha\beta) + (\frac{1}{\beta})\, ln\, t \quad (16)$$

Where α is the initial rate of adsorption (mg g-1 min-1) and β is the constant rate of desorption during the experiment. The constants are found from the slope and intercept of a linear plot of qt vs. ln(t), as shown in figs (14,17,20&23). The kinetic parameters that go with them are shown in the table (5).

The kinetic models' validity is determined by the correlation coefficients (R^2) reported in Tables 3, 4, and 5. The regression coefficients obtained from the pseudo-first-order model were greater than those obtained from the pseudo-second-order and Elovich kinetic models for MB and CV. These data show that the adsorption of MB and CV on the surface of nanoadsorbent SCMC was well followed by a pseudo-first-order process.

5. THERMODYNAMICS STUDY

It calculates how temperature affects the adsorption of both dyes (MB and CV) on nanoadsorbent SCMC. Thermodynamic parameters include entropy (ΔS^0), enthalpy (ΔH^0), and Gibbs free energy (ΔG^0), which are calculated as follows: [36]

$$\Delta G^0 = -RT\, ln\, K_L \quad (17)$$

$$ln\, K_L = \frac{\Delta S^0}{R} - \frac{\Delta H^0}{RT} \quad (18)$$

$$\Delta G^0 = \Delta H^0 - T\Delta S^0 \quad (19)$$

Where k_L is (q_e/C_e) the Langmuir constant (L/g), the gas constant is R which equal (8.314 J/mol K), and the absolute temperature is T in (K). ΔH^0 and ΔS^0 were as determined by the relationship between $\ln(k_L)$ and 1/T, as shown in Figs 24 and 25. Table 6 shows the results.

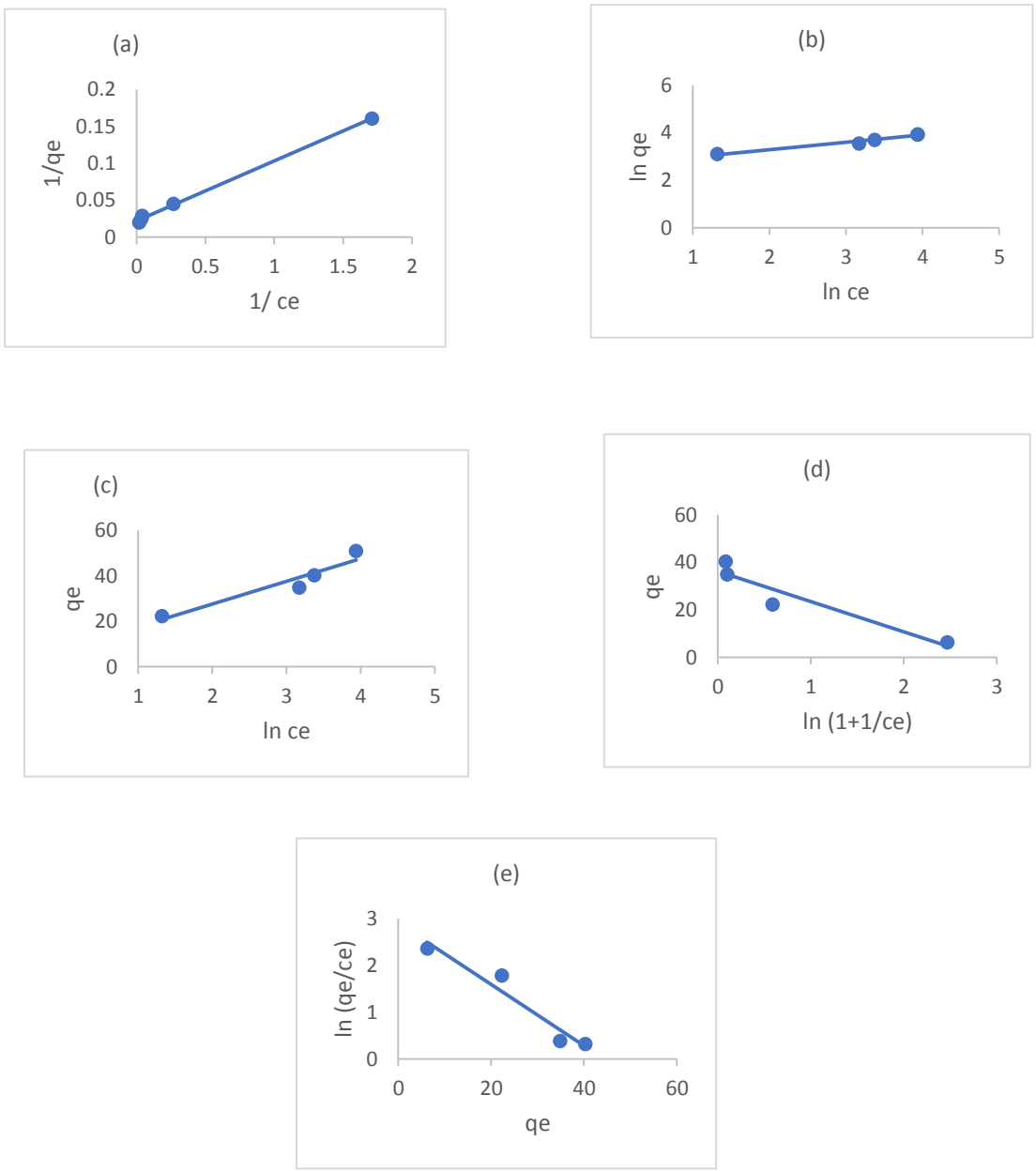

Figure 10: I.M for MB removal (a)Langmuir, (b) Freundlich, (c) Temkin, (d) D-R, (e) Elovich model (initial concentration 30ppm, temperature 25^0 C, pH 7, dose 0.05g).

The negative value of ΔG^0 indicates the feasibility and spontaneity of the adsorption.[36]. The values of ΔG^0 values are (-1.19242, -1.94761 and -2.70279 kJ/mol) for MB and (-5.99785, -8.46645 and -10.935 kJ/mol) for CV, which suggest that the adsorption process is physisorption,[36] and demonstrates that the adsorption of MB and CV onto the SCMC as nano adsorbent is spontaneous and thermodynamically favourable at all temperatures examined in this study. [25]

The enthalpy change (ΔH^0) for the adsorption process of MB and CV as calculated was 21.31211 kJ mol^{-1} and 67.56622 kJ mol^{-1}, respectively. This positive value of ΔH^0 indicates that the process of adsorption is endothermic. The high values of ΔH^0 are may be due to the presence of a strong bond between the adsorbent and dye molecules.[25] The entropy (ΔS^0) shows a positive value, which indicates that there was increased randomness during the process of adsorption.[37]

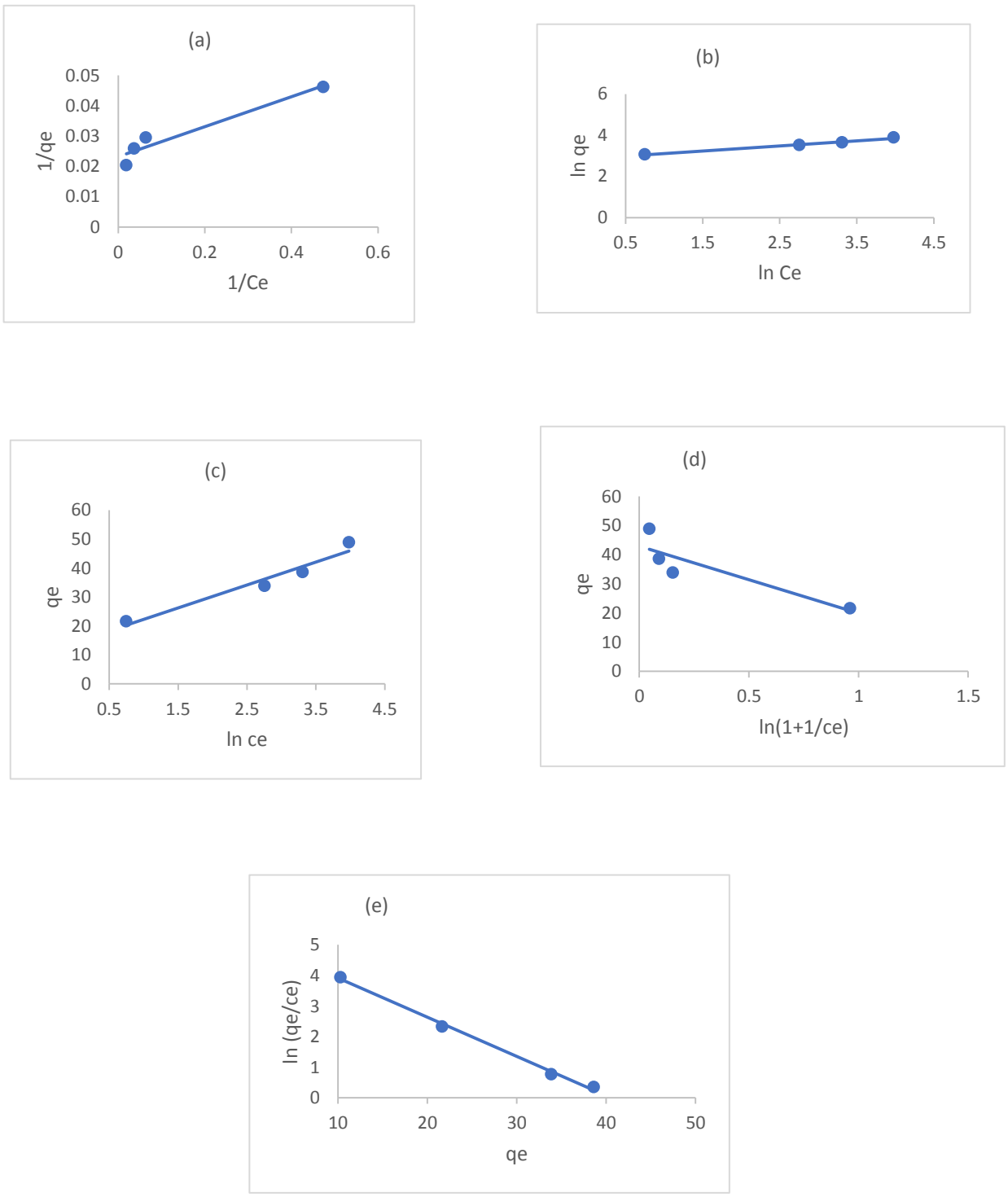

Figure 11: I.M for CV removal (a) Langmuir, (b) Freundlich, (c) Temkin, (d)D-R, (e) Elovich (initial concentration 30ppm, temperature 250 C, pH 7, dose 0.05g).

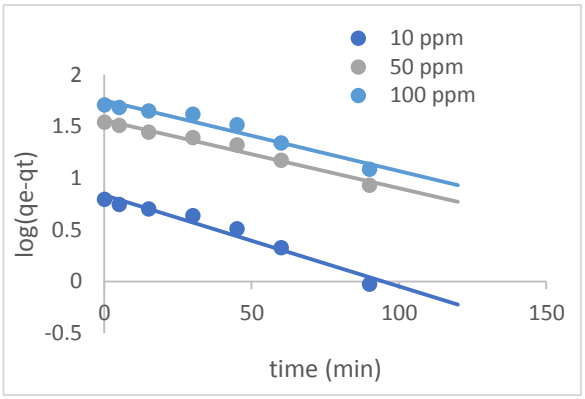

Figure 12: P.F order for MB at different concentrations (temperature 250 C, pH 7, dose 0.05g).

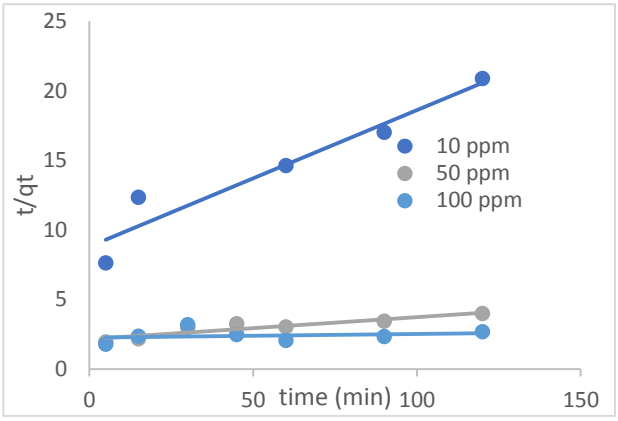

Figure 13: P.S order for MB at different concentrations (temperature 250 C, pH 7, dose 0.05g).

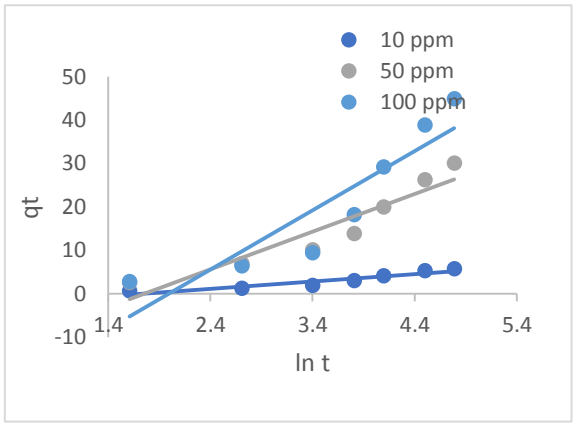

Figure 14: E.M for MB at different concentrations (temperature 250 C, pH 7, dose 0.05g).

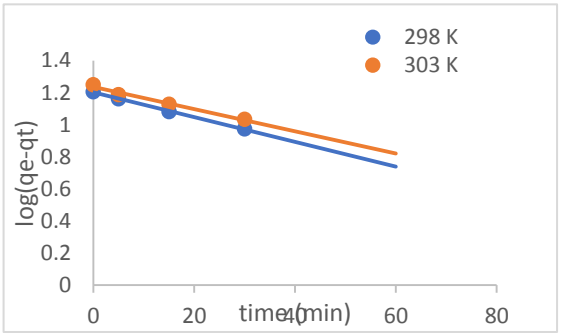

Figure 15: P. F order for MB at different temperatures (initial concentration 30 ppm, pH 7, dose 0.05g).

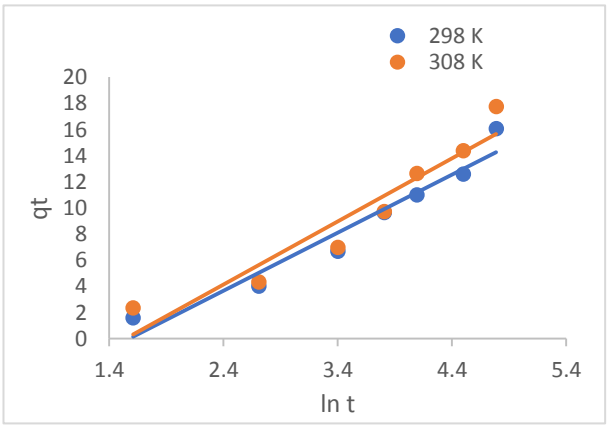

Figure 16: E. model for MB at different temperatures (initial concentration 30 ppm, pH 7, dose 0.05g).

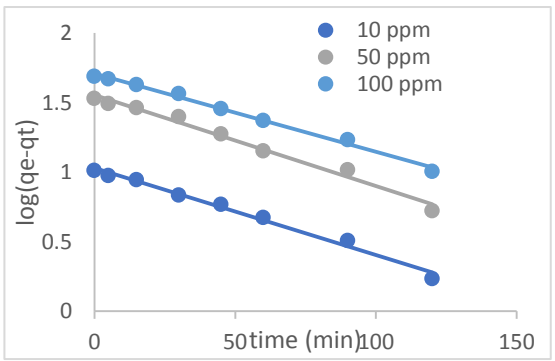

Figure 17: P.F.order for CV at different concentrations (temperature 25 0 C, pH 7, dose 0.05g).

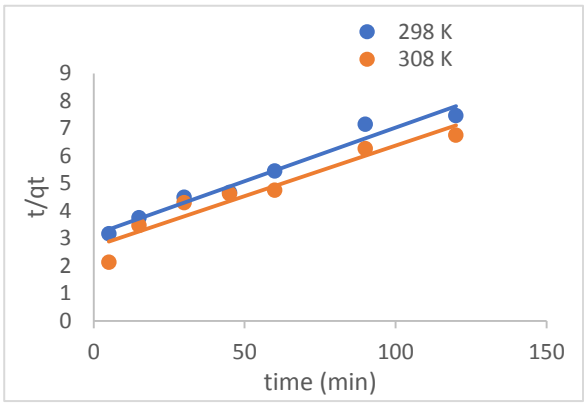

Figure 18: P.S. order for MB at different temperatures (initial concentration 30 ppm, pH 7, dose 0.05g).

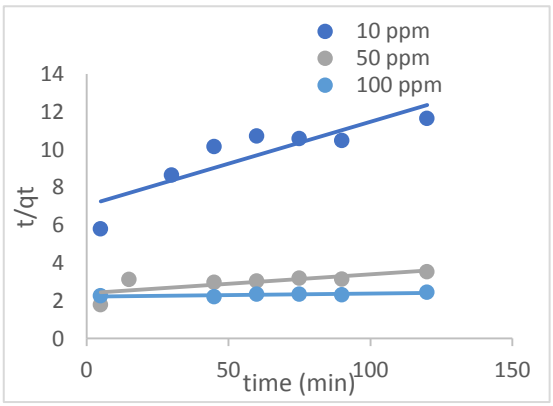

Figure 19: P.S.order for CV at different concentrations (temperature 25 0 C, pH 7, dose 0.05g).

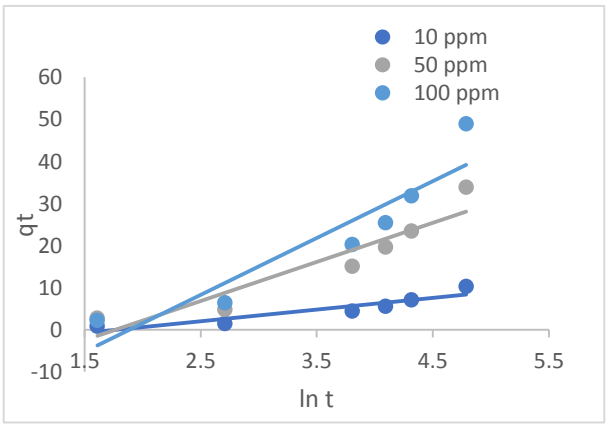

Figure 20: E. model for CV at different concentrations (temperature 25 0 C, pH 7, dose 0.05g).

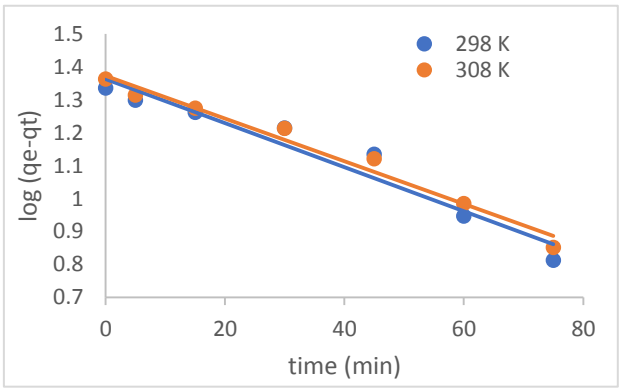

Figure 21: P.F order for CV at different temperatures (initaial concentration 30ppm, pH 7, dose 0.05g).

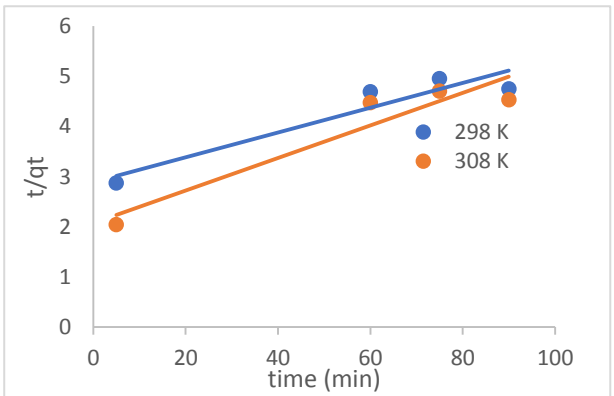

Figure 22: P.S order for CV at different tempertures (initaial concentration 30ppm, pH 7, dose 0.05g).

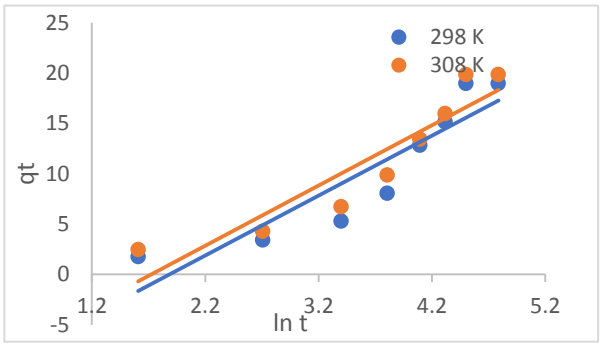

Figure 23: E.modell for CV at different temperatures (initial concentration 30ppm, pH 7, dose 0.05g).

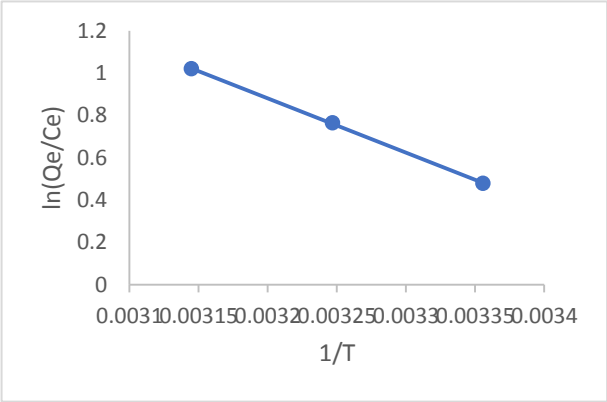

Figure 24: Thermodynamic for MB (initaial concentration 30ppm, pH 7, dose 0.05g).

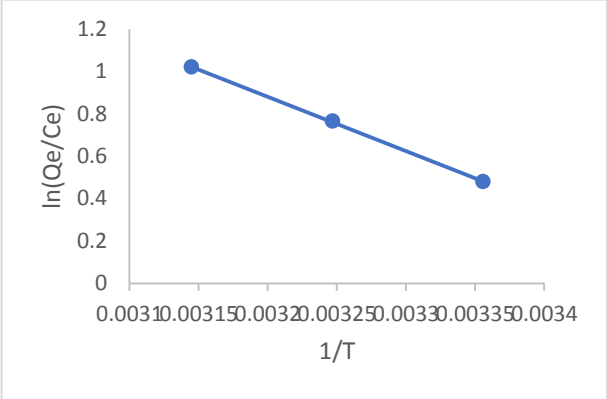

Figure 25: Thermodynamic for MB (initaial concentration 30ppm, pH 7, dose 0.05g).

6. REUSABILITY TEST

The regeneration of adsorbent is one of the most essential economic and cost-effective parameters for practical applications. The reusability of an adsorbent is proportional to its stability. As depicted in Fig. 26, the MB removal efficiency decreased progressively as regeneration cycles increased. [38]

Table 2. Calculated parameters of different isotherm models for MB and CV removal from water using SCMC.

Isotherm Model	Calculated Parameter		
		MB	CV
Langmuir	q_m (mg.g^{-1})	45.24887	43.10345
	K_L (L.mg^{-1})	0.272503	0.470588
	R_L	0.110390196	0.068640649
	R^2	0.998	0.9332
Freundlich	n	3.193868	4.084967
	K_F[(mg/g)(mg/L)^n]	14.25061	17.72365
	R^2	0.9681	0.9896
Elovich	K_E (L.mg^{-1})	1.204688	23.20099
	q_m	15.2439	7.788162
	R^2	0.9383	0.9961
Dubinin-Radushkevich	q_D (mg.g^{-1})	5.05928E+15	4.37746E+18
	B	6.338	11.475
	E (KJ.mol^{-2})	0.280872	0.208741
	R^2	0.8978	0.7751
Temkin	A	2.109185	6.188387
	B	10.032	7.912
	R^2	0.907	0.9472

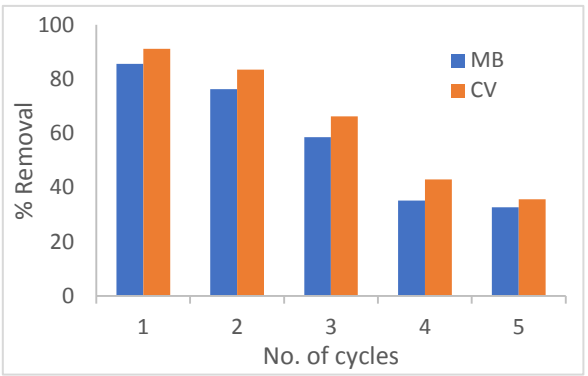

Figure 26: reusability test of SCMC

7. COMPARISON WITH OTHER STUDIES

As shown in table 7 comparison between different methods for wastewater treatment based on literatures. Table 8 showed the adsorption process of methylene blue and crystal violet dyes using SCMC nanoparticles was co mpared to previously published research.

8. CONCLUSION

This work used nanoparticles of modified carboxymethyl cellulose (SCMC) to remove the cationic dyes methylene blue and crystal violet from aqueous solutions under diverse operating parameters, including adsorbent quantity, pH, contact time, and temperature. FT-IR, SEM, TEM, and zeta potential characterise SCMC. TEM measured nanoparticles. The working parameters were examined, and the removal percentage increased with contact time and adsorbent, but the

removal decreased with increasing dye concentration. However, a neutral pH removed both dyes the best. The results shows that the maximum adsorption capacity of SCMC for the removal of MB and CV dyes are 45 mg/g and 43 mg/g, respectively.

Adsorption pseudo-first-order kinetics. The Langmuir isotherm confirmed monolayer adsorption. The change in activation enthalpy (ΔH^0), adsorption free energy (ΔG^0), and entropy (ΔS^0) were also calculated using temperature. Fundamental research will improve wastewater dye removal. Adsorption is endothermic because ΔH^0 is positive. Adsorption increases unpredictability as the change in entropy (ΔS^0) increases. The negative Gibbs free energy shift (ΔG^0) suggests spontaneous adsorption. SCMC removed wastewater CV and MB dyes well.

Table 2. Kinetic parameters calculated by Pseudo first order for MB and CV (a) at different initial concentration, (b) at different temperature.

(a) Initial oncentration (ppm)	MB			CV		
	K_1 (Lmg^{-1})	q_m(mg g^{-1})cal	R^2	K_1 (Lmg^{-1})	q_m(mg g^{-})cal	R^2
10	0.020266	6.842267	0.9644	0.014279	9.745407	0.9888
50	0.0152	36.32453	0.9765	0.01497	35.87567	0.9846
100	0.01566	56.62393	0.9497	0.012897	51.16818	0.9929

(b) Temperature (K)	MB			CV		
	K_1 (Lmg^{-1})	q_m(mg g^{-1})cal	R^2	K_1 (Lmg^{-1})	q_m(mg g^{-1})cal	R^2
298	0.0177331	15.91109248	0.9985	0.0154301	23.05154294	0.9468
308	0.015891	17.21076	0.9845	0.01497	23.61022	0.977

Table 3. Kinetic parameters calculated by Pseudo second order for MB and CV (a) at different initial concentration,

(a)Initial Concentration (ppm)	MB			CV		
	K_2(g mg^{-1} min^{-1})	q_m(mg g^{-1})cal	R^2	K_2(g mg^{-1} min^{-1})	q_m(mg g^{-1})cal	R^2
10	0.001093	10.19368	0.9242	0.000277	22.62443	0.763
50	0.000118	62.89308	0.8561	4.17484E-05	100	0.5523
100	2.98376E-06	384.6153846	0.0572	1.15237E-06	625	0.614

(b)Temperature (K)	MB			CV		
	K_2 (g mg^{-1} min^{-1})	q_m(mg g^{-1})cal	R^2	K_2 (g mg^{-1} min^{-1})	q_m(mg g^{-})cal	R^2
298	0.000484796	25.64102564	0.969	0.000210936	40.48582996	0.8939
308	0.000498	27.24796	0.9233	0.00050669	30.86419753	0.8973

Table 4. Kinetic parameters calculated by Elovich model for MB and CV (a) at different initial concentration, (b) at different temperature.

(a)Initial concentration (ppm)	MB			CV		
	α (mg g^{-1} min^{-1})	β (g mg^{-1})	R^2	α (mg g^{-1} min^{-1})	β (g mg^{-1})	R^2
10	9.41676	0.58924	0.8846	16.31047	0.360101	0.8576
50	50.24067	0.115073	0.8872	54.45455245	0.107607877	0.8744
100	99.78687998	0.073308408	0.8278	88.84209023	0.074107011	0.8611

(b) at different temperature.

(b)Temperature (K)	MB			CV		
	α (mg g^{-1} min^{-1})	β (g mg^{-1})	R^2	α (mg g^{-1} min^{-1})	β (g mg^{-1})	R^2
298	21.4972934	0.22538259	0.9429	33.54179	0.167098	0.8641
308	22.552858	0.207301146	0.9155	39.16579551	0.167883824	0.8357

Table 05. Thermodynamic for MB & CV removal.

Van't Hoff Equation						
Temperatures, K	ΔG, kJ/mol		ΔH, kJ/mol		ΔS, J/mol·K	
	MB	CV	MB	CV	MB	CV
298	-1.19242	-5.99785	21.31211	67.56622	0.075519	0.246859
303	-1.94761	-8.46645				
318	-2.70279	-10.935				

Table 6. Comparison between different removal methods.

Method	Advantages	Disadvantages
Electro Fenton Process[39]	Simple equipment High rate of reaction Low cost	Small operating limits Complex requirements of process Low conductivity
Electrolysis[40]	Low running cost	Consumption a lot of power
Ozonation [41]	Effective for gases	High cost Short lifetime
Biological process[41]	No environmental pollution	Production of sludge Long process time Limiting range of temperature
Ion exchange[42]	High removal efficiency	expensive
Reverse osmosis[42]	High removal of metals	Fouling of membrane High cost
Coagulation[43]	High efficiency	Sludge formation Undesirable products More expensive coagulants
adsorption[44]	High quality Low cost High removal percent at different concentrations	Need to regenerate adsorbent Different adsorption removal

Table 7. Comparison between different adsorbents for MB and CV removal.

Adsorbent	Dye	Qm max adsorption capacity
Activated carbon	CV	4.00 [45]
CMC/kC/AMMT composite beads	MB	10.75 [19]
Lignin-chitosan	MB	36.3 [46]
activated charcoal	CV	24.0 [47]
Olive stone activated carbon	MB	4.8–12.4 [48]
Magadiite-chitosan composite bead	MB	45.25 [49]
Bituminous schists	MB	40.82 [49]
Biosilica/alginate nanobiocomposite	CV	21.32 [50]
Calcium alginate beads	CV	29 [50]
Cellulose capped Fe3O4 nanofluids	CV	19.49 [51]
Olive stone activated carbon	MB	4.8–12.4[48]
Nano SCMC	MB	45 (present study)
Nano SCMC	CV	43 (present study)

9. REFERENCES

[1] P. Sharma, M. K. Singh, and M. S. Mehata, "Sunlight-driven MoS2 nanosheets mediated degradation of dye (crystal violet) for wastewater treatment," J. Mol. Struct., vol. 1249, pp. 1–11, 2022, doi: 10.1016/j.molstruc.2021.131651.

[2] A. Kausar et al., "Cellulose, clay and sodium alginate composites for the removal of methylene blue dye: Experimental and DFT studies," Int. J. Biol. Macromol., vol. 209, no. March, pp. 576–585, 2022, doi: 10.1016/j.ijbiomac.2022.04.044.

[3] H. Liu, X. Tian, X. Xiang, and S. Chen, "Preparation of carboxymethyl cellulose/graphene composite aerogel beads and their adsorption for methylene blue," Int. J. Biol. Macromol., vol. 202, no. September 2021, pp. 632–643, 2022, doi: 10.1016/j.ijbiomac.2022.01.052.

[4] O. Sacco et al., "Crystal violet and toxicity removal by adsorption and simultaneous photocatalysis in a continuous flow micro-reactor," Sci. Total Environ., vol. 644, pp. 430–438, 2018, doi: 10.1016/j.scitotenv.2018.06.388.

[5] C. Y. Chen, J. T. Kuo, H. A. Yang, and Y. C. Chung, "A coupled biological and photocatalysis pretreatment system for the removal of crystal violet from wastewater," Chemosphere, vol. 92, no. 6, pp. 695–701, 2013, doi: 10.1016/j.chemosphere.2013.04.040.

[6] A. salah omer et al., "Adsorption of crystal violet

and methylene blue dyes using a cellulose-based adsorbent from sugercane bagasse: characterization, kinetic and isotherm studies," J. Mater. Res. Technol., vol. 19, pp. 3241–3254, 2022, doi: 10.1016/j.jmrt.2022.06.045.

[7] A. Putranto et al., "Effects of pyrolysis temperature and impregnation ratio on adsorption kinetics and isotherm of methylene blue on corn cobs activated carbons," South African J. Chem. Eng., vol. 42, no. July, pp. 91–97, 2022, doi: 10.1016/j.sajce.2022.07.008.

[8] X. Hu et al., "Simple synthesis of the novel adsorbent BaCO3/g-C3N4 for rapid and high-efficient selective removal of Crystal Violet," Colloids Surfaces A Physicochem. Eng. Asp., vol. 600, no. March, p. 124948, 2020, doi: 10.1016/j.colsurfa.2020.124948.

[9] A. H. Alibak, M. Khodarahmi, P. Fayyazsanavi, S. M. Alizadeh, A. J. Hadi, and E. Aminzadehsarikhanbeglou, "Simulation the adsorption capacity of polyvinyl alcohol/carboxymethyl cellulose based hydrogels towards methylene blue in aqueous solutions using cascade correlation neural network (CCNN) technique," J. Clean. Prod., vol. 337, no. January, p. 130509, 2022, doi: 10.1016/j.jclepro.2022.130509.

[10] C. Liu, A. M. Omer, and X. kun Ouyang, "Adsorptive removal of cationic methylene blue dye using carboxymethyl cellulose/k-carrageenan/activated montmorillonite composite beads: Isotherm and kinetic studies," Int. J. Biol. Macromol., vol. 106, pp. 823–833, 2018, doi: 10.1016/j.ijbiomac.2017.08.084.

[11] L. Boughrara, F. Zaoui, M. Guezzoul, F. Z. Sebba, B. Bounaceur, and S. O. Kada, "New alginic acid derivatives ester for methylene blue dye adsorption: kinetic, isotherm, thermodynamic, and mechanism study," Int. J. Biol. Macromol., vol. 205, no. January, pp. 651–663, 2022, doi: 10.1016/j.ijbiomac.2022.02.087.

[12] M. Luo et al., "Super-assembled highly compressible and flexible cellulose aerogels for methylene blue removal from water," Chinese Chem. Lett., vol. 32, no. 6, pp. 2091–2096, 2021, doi: 10.1016/j.cclet.2021.03.024.

[13] T. Zhu et al., "Preparation of an amphoteric adsorbent from cellulose for wastewater treatment," React. Funct. Polym., vol. 169, no. October, p. 105086, 2021, doi: 10.1016/j.reactfunctpolym.2021.105086.

[14] Z. Sun et al., "A novel modified carboxymethyl cellulose hydrogel adsorbent for efficient removal of poisonous metals from wastewater: Performance and mechanism," J. Environ. Chem. Eng., vol. 10, no. 4, p. 108179, 2022, doi: 10.1016/j.jece.2022.108179.

[15] B. Deka, D. Mohanta, and A. Saha, "Featuring exfoliated 2D stacks into fractal-like patterns in WS2/carboxy methyl cellulose nanocomposites," Surfaces and Interfaces, vol. 29, no. January, p. 101727, 2022, doi: 10.1016/j.surfin.2022.101727.

[16] M. Tanzifi et al., "Carboxymethyl cellulose improved adsorption capacity of polypyrrole/CMC composite nanoparticles for removal of reactive dyes: Experimental optimization and DFT calculation," Chemosphere, vol. 255, 2020, doi: 10.1016/j.chemosphere.2020.127052.

[17] S. Rani and S. Chaudhary, "Adsorption of methylene blue and crystal violet dye from waste water using Citrus limetta peel as an adsorbent," Mater. Today Proc., no. xxxx, pp. 1–9, 2022, doi: 10.1016/j.matpr.2022.01.237.

[18] H. Li, H. Shi, Y. He, X. Fei, and L. Peng, "Preparation and characterization of carboxymethyl cellulose-based composite films reinforced by cellulose nanocrystals derived from pea hull waste for food packaging applications," Int. J. Biol. Macromol., vol. 164, pp. 4104–4112, 2020, doi: 10.1016/j.ijbiomac.2020.09.010.

[19] A. S. Eltaweil, G. S. Elgarhy, G. M. El-Subruiti, and A. M. Omer, "Carboxymethyl cellulose/carboxylated graphene oxide composite microbeads for efficient adsorption of cationic methylene blue dye," Int. J. Biol. Macromol., vol. 154, pp. 307–318, 2020, doi: 10.1016/j.ijbiomac.2020.03.122.

[20] M. F. Elkady et al., "Nano-sulphonated poly (glycidyl methacrylate) cations exchanger for cadmium ions removal: Effects of operating parameters," Desalination, vol. 279, no. 1–3, pp. 152–162, 2011, doi: 10.1016/j.desal.2011.06.002.

[21] M. M. Wang and L. Wang, "Synthesis and characterization of carboxymethyl cellulose/organic montmorillonite nanocomposites and its adsorption behavior for Congo Red dye," Water Sci. Eng., vol. 6, no. 3, pp. 272–282, 2013, doi: 10.3882/j.issn.1674-2370.2013.03.004.

[22] Z. Moradi, A. Alihosseini, and A. Ghadami, “Adsorption removal of arsenic from Aqueous solution by carboxy methyl Cellulose(CMC) modified with montmorillonite,” Results Mater., vol. 17, no. January, p. 100378, 2023, doi: 10.1016/j.rinma.2023.100378.

[23] V. Singh, S. Joshi, and T. Malviya, “Carboxymethyl cellulose-rosin gum hybrid nanoparticles: An efficient drug carrier,” Int. J. Biol. Macromol., vol. 112, pp. 390–398, 2018, doi: 10.1016/j.ijbiomac.2018.01.184.

[24] T. Aziz et al., “Synthesis, characterization and adsorption behavior of modified cellulose nanocrystals towards different cationic dyes,” Chemosphere, vol. 321, no. January, p. 137999, 2023, doi: 10.1016/j.chemosphere.2023.137999.

[25] L. Borah, M. Goswami, and P. Phukan, “Adsorption of methylene blue and eosin yellow using porous carbon prepared from tea waste: Adsorption equilibrium, kinetics and thermodynamics study,” J. Environ. Chem. Eng., vol. 3, no. 2, pp. 1018–1028, 2015, doi: 10.1016/j.jece.2015.02.013.

[26] V. Javanbakht and Z. Rafiee, “Fibrous polyester sponge modified with carboxymethyl cellulose and Zeolitic imidazolate frameworks for methylene blue dye removal in batch and continuous adsorption processes,” J. Mol. Struct., vol. 1249, p. 131552, 2022, doi: 10.1016/j.molstruc.2021.131552.

[27] M. N. Nimbalkar and B. R. Bhat, “Journal of Environmental Chemical Engineering Simultaneous adsorption of methylene blue and heavy metals from water using Zr-MOF having free carboxylic group,” J. Environ. Chem. Eng., vol. 9, no. 5, p. 106216, 2021, doi: 10.1016/j.jece.2021.106216.

[28] A. A. Emam, S. A. Abo Faraha, F. H. Kamal, A. M. Gamal, and M. Basseem, “Modification and characterization of Nano cellulose crystalline from Eichhornia crassipes using citric acid: An adsorption study,” Carbohydr. Polym., vol. 240, no. December 2019, p. 116202, 2020, doi: 10.1016/j.carbpol.2020.116202.

[29] C. Muthukumaran, V. M. Sivakumar, and M. Thirumarimurugan, “Adsorption isotherms and kinetic studies of crystal violet dye removal from aqueous solution using surfactant modified magnetic nanoadsorbent,” J. Taiwan Inst. Chem. Eng., vol. 63, pp. 354–362, 2016, doi: 10.1016/j.jtice.2016.03.034.

[30] S. Patra, E. Roy, R. Madhuri, and P. K. Sharma, “Agar based bimetallic nanoparticles as high-performance renewable adsorbent for removal and degradation of cationic organic dyes,” J. Ind. Eng. Chem., vol. 33, pp. 226–238, 2016, doi: 10.1016/j.jiec.2015.10.008.

[31] S. Sultana et al., “Adsorption of crystal violet dye by coconut husk powder: Isotherm, kinetics and thermodynamics perspectives,” Environ. Nanotechnology, Monit. Manag., vol. 17, no. January, p. 100651, 2022, doi: 10.1016/j.enmm.2022.100651.

[32] M. F. Mubarak, A. M. Zayed, and H. A. Ahmed, “Activated Carbon/Carborundum@Microcrystalline Cellulose core shell nano-composite: Synthesis, characterization and application for heavy metals adsorption from aqueous solutions,” Ind. Crops Prod., vol. 182, no. January, p. 114896, 2022, doi: 10.1016/j.indcrop.2022.114896.

[33] Z. Wu et al., “Synthesis, characterization, and methylene blue adsorption of multiple-responsive hydrogels loaded with Huangshui polysaccharides, polyvinyl alcohol, and sodium carboxyl methyl cellulose,” Int. J. Biol. Macromol., vol. 216, no. February, pp. 157–171, 2022, doi: 10.1016/j.ijbiomac.2022.06.178.

[34] I. Mobasherpour, E. Salahi, and M. Pazouki, “Removal of divalent cadmium cations by means of synthetic nano crystallite hydroxyapatite,” Desalination, vol. 266, no. 1–3, pp. 142–148, 2011, doi: 10.1016/j.desal.2010.08.016.

[35] M. S. Thabet and A. M. Ismaiel, “Sol-Gel <i>γ</i>-Al₂O₃ Nanoparticles Assessment of the Removal of Eosin Yellow Using: Adsorption, Kinetic and Thermodynamic Parameters,” J. Encapsulation Adsorpt. Sci., vol. 06, no. 03, pp. 70–90, 2016, doi: 10.4236/jeas.2016.63007.

[36] T. Liu et al., “Adsorption of methylene blue from aqueous solution by graphene,” Colloids Surfaces B Biointerfaces, vol. 90, no. 1, pp. 197–203, 2012, doi: 10.1016/j.colsurfb.2011.10.019.

[37] S. R. Shirsath, A. P. Patil, B. A. Bhanvase, and S. H. Sonawane, “Ultrasonically prepared poly(acrylamide)-kaolin composite hydrogel for removal of crystal violet dye from wastewater,” J. Environ. Chem. Eng., vol. 3, no. 2, pp. 1152–1162, 2015, doi: 10.1016/j.jece.2015.04.016.

[38] M. U. Rehman et al., “Physicochemical

characterization of Pakistani clay for adsorption of methylene blue: Kinetic, isotherm and thermodynamic study," Mater. Chem. Phys., vol. 269, no. May, p. 124722, 2021, doi: 10.1016/j.matchemphys.2021.124722.

[39] G. Bal and A. Thakur, "Distinct approaches of removal of dyes from wastewater: A review," Mater. Today Proc., vol. 50, no. xxxx, pp. 1575–1579, 2021, doi: 10.1016/j.matpr.2021.09.119.

[40] W. Fawcett-Hirst, T. J. Temple, M. K. Ladyman, and F. Coulon, "A review of treatment methods for insensitive high explosive contaminated wastewater," Heliyon, vol. 7, no. 7, p. e07438, 2021, doi: 10.1016/j.heliyon.2021.e07438.

[41] A. K. Verma, R. R. Dash, and P. Bhunia, "A review on chemical coagulation/flocculation technologies for removal of colour from textile wastewaters," J. Environ. Manage., vol. 93, no. 1, pp. 154–168, 2012, doi: 10.1016/j.jenvman.2011.09.012.

[42] R. M. El-taweel et al., "ur of," Curr. Res. Green Sustain. Chem., p. 100358, 2023, doi: 10.1016/j.crgsc.2023.100358.

[43] A. Kumar, N. K. Srivastava, and P. Gera, "Removal of color from pulp and paper mill wastewater- methods and techniques- A review," J. Environ. Manage., vol. 298, no. August, p. 113527, 2021, doi: 10.1016/j.jenvman.2021.113527.

[44] D. Jyoti, R. Sinha, and C. Faggio, "Advances in biological methods for the sequestration of heavy metals from water bodies: A review," Environ. Toxicol. Pharmacol., vol. 94, no. February, p. 103927, 2022, doi: 10.1016/j.etap.2022.103927.

[45] F. Shojaeipoor, B. Masoumi, M. H. Banakar, and J. Rastegar, "Aminopropyl-containing ionic liquid based organosilica as a novel and efficient adsorbent for removal of crystal violet from wastewaters," Chinese J. Chem. Eng., vol. 25, no. 9, pp. 1294–1302, 2017, doi: 10.1016/j.cjche.2016.09.003.

[46] M. Yan, W. Huang, and Z. Li, "Chitosan cross-linked graphene oxide/lignosulfonate composite aerogel for enhanced adsorption of methylene blue in water," Int. J. Biol. Macromol., vol. 136, pp. 927–935, 2019, doi: 10.1016/j.ijbiomac.2019.06.144.

[47] M. R. Hassan, S. M. Yakout, A. A. Abdeltawab, and M. I. Aly, "Ultrasound facilitates and improves removal of triphenylmethane (crystal violet) dye from aqueous solution by activated charcoal: A kinetic study," J. Saudi Chem. Soc., vol. 25, no. 6, p. 101231, 2021, doi: 10.1016/j.jscs.2021.101231.

[48] E. Misran, O. Bani, E. M. Situmeang, and A. S. Purba, "Banana stem based activated carbon as a low-cost adsorbent for methylene blue removal: Isotherm, kinetics, and reusability," Alexandria Eng. J., vol. 61, no. 3, pp. 1946–1955, 2022, doi: 10.1016/j.aej.2021.07.022.

[49] A. H. Jawad, S. E. M. Saber, A. S. Abdulhameed, A. Reghioua, Z. A. ALOthman, and L. D. Wilson, "Mesoporous activated carbon from mangosteen (Garcinia mangostana) peels by H3PO4 assisted microwave: Optimization, characterization, and adsorption mechanism for methylene blue dye removal," Diam. Relat. Mater., vol. 129, no. June, 2022, doi: 10.1016/j.diamond.2022.109389.

[50] H. Najafi, N. Asasian-Kolur, and S. Sharifian, "Adsorption of chromium(VI) and crystal violet onto granular biopolymer-silica pillared clay composites from aqueous solutions," J. Mol. Liq., vol. 344, p. 117822, 2021, doi: 10.1016/j.molliq.2021.117822.

[51] P. Kumbhar, D. Narale, R. Bhosale, C. Jambhale, J. H. Kim, and S. Kolekar, "Synthesis of tea waste/Fe3O4magnetic composite (TWMC) for efficient adsorption of crystal violet dye: Isotherm, kinetic and thermodynamic studies," J. Environ. Chem. Eng., vol. 10, no. 3, p. 107893, 2022, doi: 10.1016/j.jece.2022.107893.